

A primer on elliptic functions with applications in classical mechanics

Alain J Brizard

Department of Chemistry and Physics, Saint Michael's College, Colchester, VT 05439, USA

Received 2 December 2008, in final form 2 February 2009

Published 8 May 2009

Online at stacks.iop.org/EJP/30/729

Abstract

The Jacobi and Weierstrass elliptic functions used to be part of the standard mathematical arsenal of physics students. They appear as solutions of many important problems in classical mechanics: the motion of a planar pendulum (Jacobi), the motion of a force-free asymmetric top (Jacobi), the motion of a spherical pendulum (Weierstrass) and the motion of a heavy symmetric top with one fixed point (Weierstrass). The planar pendulum can, in fact, be used to highlight an important connection between the Jacobi and Weierstrass elliptic functions. The easy access to mathematical software by physics students suggests that they might reappear as useful mathematical tools in the undergraduate curriculum.

1. Introduction

A long time ago, physics students were well trained in applications of elliptic functions in solving a great variety of problems in classical mechanics. For example, Whittaker's *Treatise on the Analytical Dynamics of Particles and Rigid Bodies* [1] appears to implicitly assume that the reader is fully conversant with the theory of elliptic functions.

Elliptic functions rapidly fell out the standard physics curriculum over the past fifty years, however, and they are now only mentioned in passing in most standard (modern) textbooks on classical mechanics [2–4]. The information on these mythical functions is now relegated to mathematics textbooks [5, 6] and mathematical handbooks [7, 8] with notations and conventions that are often contradictory or difficult to understand by physicists. The purpose of this paper is thus to (re)introduce the Jacobi and Weierstrass elliptic functions to a new generation of physics students through a series of standard problems found in classical mechanics [9].

Many problems in classical mechanics involve calculating of one of the following integrals [3]. First, the time integral

$$t(x) = \pm \int_{x_0}^x \frac{dy}{\sqrt{(2/m)[E - U(y)]}} \quad (1)$$

arises in solutions $x(t)$ of one-dimensional problems associated with motion of a particle of mass m and constant total energy E in a time-independent potential $U(x)$, where the initial condition x_0 may be chosen to correspond to a root of the turning-point equation $E = U(x_0)$. Next, the orbit integral

$$\theta(s) = \pm \int_{s_0}^s \frac{d\sigma}{\sqrt{(2\mu/\ell^2)[E - U(\sigma^{-1}) - \ell^2\sigma^2/2\mu]}} \quad (2)$$

arises in solutions $r(\theta) \equiv 1/s(\theta)$ of central-force problems involving the motion of a (fictitious) particle of (reduced) mass μ , with constant total energy E and angular momentum $\ell = \mu r^2 \dot{\theta}$, in a central potential $U(r)$, where the initial condition $s(0) = s_0$ is a turning point where $E = U(s_0^{-1}) - \ell^2 s_0^2 / 2\mu$. Lastly, the time integral

$$t(\theta) = \pm \int_{\cos \theta_0}^{\cos \theta} \frac{du}{\sqrt{(2/I_1)(1 - u^2)[E - V(u)]}} \quad (3)$$

arises in solutions $\theta(t)$ of rigid-body dynamics in the Lagrangian representation, where I_1 denotes one principal component of the inertia tensor for a symmetric top ($I_1 = I_2 \neq I_3$), the effective potential $V(\cos \theta)$ contains terms associated with conserved angular momenta associated with the ignorable Eulerian angles ψ and φ , and the initial condition $\theta(0) = \theta_0$ is a turning point where $E = V(\cos \theta_0)$.

Exact analytical solutions for these integrals exist only for certain potentials, in which cases the inversions $t(x) \rightarrow x(t)$, $\theta(s) \rightarrow s(\theta)$ and $t(\theta) \rightarrow \theta(t)$ can be expressed in terms of known functions. For example, exact solutions of the time integral (1) exist in terms of trigonometric (or singly periodic) functions when the potential $U(x)$ is a quadratic polynomial in x . Trigonometric solutions of the orbit integral (2), on the other hand, exist for the Kepler problem $U(r) = -k/r$ and the isotropic harmonic oscillator $U(r) = kr^2/2$. The purpose of this paper is to explore exact analytic solutions of the integrals (1)–(3) expressed in terms of doubly periodic functions called elliptic functions [6]. For example, exact solutions of the orbit integral (2) for the central potential $U(r) = kr^n$ exist in terms of elliptic functions [1] for $n = \pm 6, \pm 4, 1$ and -3 . The time integral (3), on the other hand, has a solution in terms of elliptic functions for the problem of the heavy symmetric top (of mass M) with one fixed point (located at a distance h from the center of mass), where the gravitational potential is $V(\cos \theta) = Mgh \cos \theta$.

1.1. Doubly periodic elliptic functions

We now present a brief definition of elliptic functions in terms of their analytic (complex) properties. A function $F(z)$ is said to be doubly periodic, with periods η and η' (where the complex-valued ratio η'/η has a positive-definite imaginary part), if $F(z + m\eta + n\eta') = F(z)$, for $m, n = 0, \pm 1, \pm 2, \dots$ (but not $m = 0 = n$). We note that, in the limit $|\eta'| \rightarrow \infty$ (assuming that η is real), the function $F(z)$ becomes singly periodic with period η . The *fundamental period-parallelogram* of a doubly periodic function is defined by the quadrangle formed by the four points $(0, \eta, \eta', \eta + \eta')$. Within this fundamental parallelogram, elliptic functions are doubly periodic functions with two simple zeros and either a second-order pole (Weierstrass elliptic function) or two first-order poles (Jacobi elliptic function). Note that there are no elliptic functions of first order and that there are no multiply periodic functions with more than two periods [6].

Elliptic functions $y(x; \mathbf{a})$ are defined as solutions of the nonlinear ordinary differential equation

$$\left(\frac{dy}{dx}\right)^2 = a_4 y^4 + a_3 y^3 + a_2 y^2 + a_1 y + a_0,$$

where $\mathbf{a} \equiv (a_0, a_1, \dots, a_4)$ are constant coefficients. This equation can be formally solved by finding the inverse function

$$x(y; \mathbf{a}) = x_0 \pm \int_{y_0(\mathbf{a})}^y \frac{ds}{\sqrt{a_4 s^4 + a_3 s^3 + a_2 s^2 + a_1 s + a_0}},$$

where $y_0(\mathbf{a})$ is a root of the quartic polynomial $a_4 y^4 + a_3 y^3 + a_2 y^2 + a_1 y + a_0$ and $x(y_0; \mathbf{a}) = x_0$. Jacobi elliptic functions are defined in terms of the quartic polynomial $(1 - y^2)(a + by^2)$, where a and b are constants, while Weierstrass elliptic functions are defined in terms of the cubic polynomial $4y^3 - g_2 y - g_3$, where g_2 and g_3 are constants. There is a connection between the Jacobi and Weierstrass elliptic functions [6] that will be exploited later in section 3.1 (see also appendices A and B).

1.2. Organization

The remainder of the paper is organized as follows. In section 2, we present the Jacobi elliptic functions and discuss, first, the Seiffert spherical spiral [6, 10] as a mathematical introduction of their doubly periodic nature. Next, we discuss exact solutions to the physical problems of (i) the planar pendulum and (ii) Euler's equations for a force-free asymmetric top. In section 3, we present the Weierstrass elliptic functions and discuss exact solutions to the physical problems of (i) the planar pendulum, (ii) the spherical pendulum and (iii) the motion of a heavy symmetric top with one fixed point. The fact that the problem of the planar pendulum is solved in terms of the Jacobi and Weierstrass elliptic functions highlights an important connection between these functions. In section 4, we discuss one interesting application of elliptic functions in terms of the travelling-wave solutions of nonlinear partial differential equations. We summarize our work in section 5 and present mathematical details in appendices A and B. Lastly, we note that the notation used for the Jacobi and Weierstrass elliptic functions in our paper is partly based on the material presented elsewhere [7–9].

2. Jacobi elliptic functions

We begin our introduction of elliptic functions with the more familiar Jacobi elliptic functions ($\text{sn } z$, $\text{cn } z$, $\text{dn } z$). First, the Jacobi elliptic function $\text{sn } z \equiv \text{sn}(z|m)$, with modulus $m < 1$, is a solution to the differential equation

$$\left(\frac{dy}{dz}\right)^2 = (1 - y^2)(1 - my^2), \quad (4)$$

subject to the initial condition $y(0) = 0$. Next, the Jacobi elliptic function $\text{cn } z \equiv \text{cn}(z|m)$, with modulus $m < 1$ and complementary modulus $m' = 1 - m > 0$, is a solution to the differential equation

$$\left(\frac{dy}{dz}\right)^2 = (1 - y^2)(my^2 + m'), \quad (5)$$

subject to the initial condition $y(0) = 1$. Lastly, the Jacobi elliptic function $\text{dn } z \equiv \text{dn}(z|m)$, with $m' = 1 - m > 0$, is a solution to the differential equation

$$\left(\frac{dy}{dz}\right)^2 = (1 - y^2)(y^2 - m'), \quad (6)$$

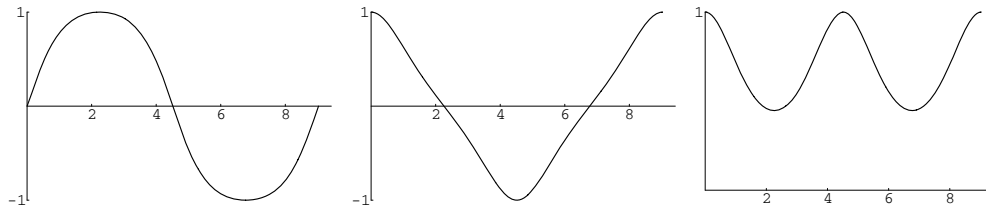


Figure 1. From left to right, plots of $\text{sn}(z|m)$, $\text{cn}(z|m)$ and $\text{dn}(z|m)$ from $z = 0$ to $4K(m)$ for $m = 4/5$.

subject to the initial condition $y(0) = 1$. The differential equations (4)–(6) imply that the Jacobi elliptic functions have the following derivatives with respect to z :

$$\left. \begin{aligned} \text{sn}'z &= \text{cn } z \text{ dn } z \\ \text{cn}'z &= -\text{sn } z \text{ dn } z \\ \text{dn}'z &= -m \text{cn } z \text{ sn } z \end{aligned} \right\}, \quad (7)$$

where the sign conventions satisfy the identities

$$\text{sn}^2(z|m) + \text{cn}^2(z|m) = 1 = \text{dn}^2(z|m) + m \text{sn}^2(z|m). \quad (8)$$

We note that, for the special case $m = 1$, the solutions to the differential equations (4)–(6) yield

$$\left. \begin{aligned} \text{sn}(z|1) &= \tanh z \\ \text{cn}(z|1) &= \text{sech } z \\ \text{dn}(z|1) &= \text{sech } z \end{aligned} \right\}, \quad (9)$$

while for $m = 0$, they yield

$$\left. \begin{aligned} \text{sn}(z|0) &= \sin z \\ \text{cn}(z|0) &= \cos z \\ \text{dn}(z|0) &= 1 \end{aligned} \right\}, \quad (10)$$

and both special cases trivially satisfy the identities (8).

The Jacobi elliptic functions ($\text{sn } z$, $\text{cn } z$, $\text{dn } z$) are doubly periodic functions of z , with real-valued periods that are either $2K$ ($\text{dn } z$) or $4K$ ($\text{sn } z$ and $\text{cn } z$) (see figure 1), where

$$K \equiv K(m) = \int_0^{\pi/2} \frac{d\theta}{\sqrt{1 - m \sin^2 \theta}} = \frac{\pi}{2} \left(1 + \frac{1}{4}m + \frac{9}{64}m^2 + \dots \right), \quad (11)$$

and purely imaginary periods that are either $2iK'$ ($\text{sn } z$) or $4iK'$ ($\text{cn } z$ and $\text{dn } z$), where

$$iK'(m) \equiv iK(m') = i \int_0^{\pi/2} \frac{d\theta}{\sqrt{1 - m' \sin^2 \theta}}. \quad (12)$$

Figure 2 shows a plot of $2K(m)/\pi = 2K'(1 - m)/\pi$ from $m = 0$ to $m = 1$, with $K(0) = \pi/2 = K'(1)$ (the horizontal dashed line in figure 2) while $K(m) = K'(1 - m) \rightarrow \infty$ as $m \rightarrow 1$. For example, $\text{sn}(z|0) = \sin z$ has a real period of $4K(0) = 2\pi$ while $\text{sn}(z|1) = \tanh z$ has an imaginary period of $2iK'(1) = i\pi$. Figure 3 shows the plots of $\text{sn } z$ and $-i \text{sn}(iz)$ for $m = 2/3$, which exhibit both a real period ($4K$) and an imaginary period ($2iK'$). The fundamental period–parallelogram for the Jacobi elliptic functions is, therefore, the rectangle with corners at $(0, 4K, 4iK', 4K + 4iK')$, where zeros occur for real values of z (at $2K$ and $4K$) while singularities occur for imaginary values of z (at iK' and $3iK'$).

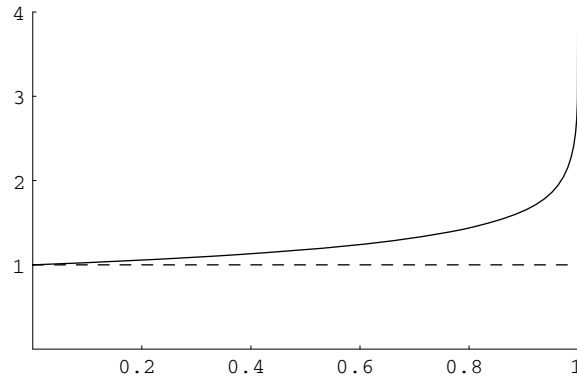


Figure 2. Plot of $2K(m)/\pi = 2K'(1-m)/\pi$ from $m = 0$ to $m = 1$.

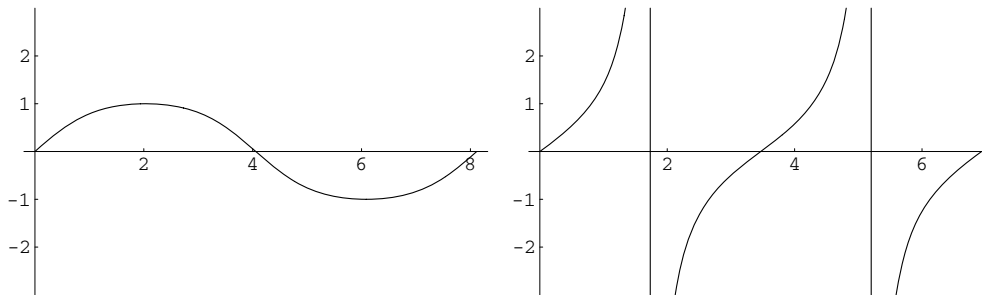


Figure 3. Plots of (left) $\text{sn}(z|m)$ from $z = 0$ to $z = 4K(m)$ for $m = 2/3$ and (right) $-i \text{sn}(iz|m)$ from $z = 0$ to $z = 4K'(m)$ for $m = 2/3$.

The Jacobi elliptic functions for $m > 1$ ($m' < 0$) are obtained from transformations of the differential equations (4)–(6) in terms of the new variable $m^{1/2}z$. Hence, for $m > 1$, we find

$$\left. \begin{aligned} \text{sn}(z|m) &= m^{-1/2} \text{sn}(m^{1/2}z|m^{-1}) \\ \text{cn}(z|m) &= \text{dn}(m^{1/2}z|m^{-1}) \\ \text{dn}(z|m) &= \text{cn}(m^{1/2}z|m^{-1}) \end{aligned} \right\}, \tag{13}$$

which satisfy identities similar to the identities (8).

2.1. Seiffert spherical spiral

A simple example that clearly exhibits the periodicity of the Jacobi elliptic functions $\text{sn } z$ and $\text{cn } z$ is given by the *Seiffert spherical spiral*, [6, 10] defined as a periodic curve on the unit sphere and constructed as follows. First, we use the cylindrical metric $ds^2 = d\rho^2 + \rho^2 d\varphi^2 + dz^2$ with $z = \sqrt{1 - \rho^2}$, and the azimuthal angle $\varphi(s) \equiv ks$ is parameterized by the arc length s (assuming that the initial point of the curve is $\rho = 0, \varphi = 0$ and $z = 1$). Hence, we readily obtain the differential equation

$$\left(\frac{d\rho}{ds}\right)^2 = (1 - \rho^2)(1 - k^2 \rho^2), \tag{14}$$

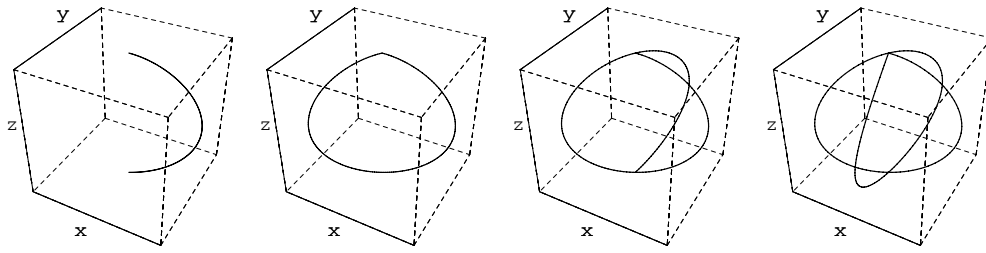


Figure 4. Three-dimensional plots of the Seiffert spherical spiral (16) on the surface of the unit sphere for $k = 0.15$ from $s = 0$ to (from left to right) $s = 2K(k^2)$, $s = 4K(k^2)$, $s = 6K(k^2)$ and $s = 8K(k^2)$.

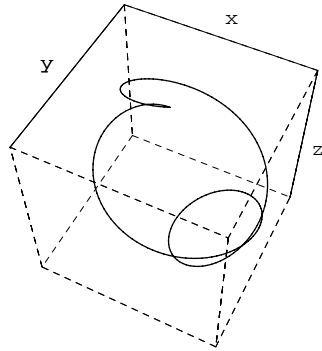


Figure 5. Seiffert spherical spiral for $k = 0.95$ from $s = 0$ to $s = 4K(k^2)$.

which leads (with $0 < m \equiv k^2 < 1$) to the solutions

$$\left. \begin{aligned} \rho(s) &= \operatorname{sn}(s|k^2) \\ z(s) &= \sqrt{1 - \rho^2(s)} = \operatorname{cn}(s|k^2) \end{aligned} \right\}, \tag{15}$$

subject to the initial conditions $\rho(0) = 0$ and $z(0) = 1$. The Seiffert spherical spiral is generated by plotting on the unit sphere the path of the unit vector

$$\widehat{r}(s) = \operatorname{sn}(s|k^2)[\cos(ks)\widehat{x} + \sin(ks)\widehat{y}] + \operatorname{cn}(s|k^2)\widehat{z} \tag{16}$$

as a function of s . Note that the identity $\operatorname{sn}^2 s + \operatorname{cn}^2 s = 1$ ensures that $|\widehat{r}| = 1$ for all values of k . Figure 4 shows the Seiffert spherical spiral for $k = 0.15$; note that at each value $4nK$ ($n = 1, 2, \dots$), the orbit returns to the initial point at $\rho = 0$ and $z = 1$. The special case $k = 0$ simply represents a great circle ($\widehat{r} = \sin s\widehat{x} + \cos s\widehat{z}$) produced by the intersection of the (x, z) -plane with the unit sphere. Figure 5 shows the complex periodic nature of the Seiffert-spiral orbit for $k = 0.95$.

Lastly, the case $k > 1$ is handled with the identities (13), so that

$$\left. \begin{aligned} \rho(s) &= k^{-1} \operatorname{sn}(ks|k^{-2}) \\ z(s) &= \sqrt{1 - \rho^2(s)} = \operatorname{dn}(ks|k^{-2}) \end{aligned} \right\}, \tag{17}$$

and the Seiffert spherical spiral is now periodic with period $4k^{-1}K(k^{-2})$.

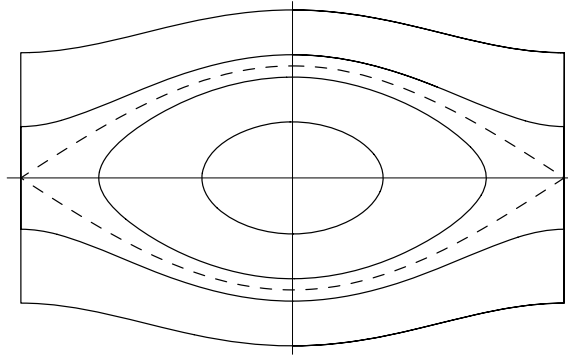


Figure 6. Phase portrait (φ' versus φ) for the planar pendulum: the bounded libration orbits (19) for $\epsilon < 2$ (inner curves) and the unbounded rotation orbits (20) for $\epsilon > 2$ (outer curves) are separated by the separatrix orbits (21) for $\epsilon = 2$ (dashed curves).

2.2. Planar pendulum

The problem of the planar pendulum [1, 2] is represented by the (normalized) differential equation

$$\left(\frac{d\varphi}{d\tau}\right)^2 = \frac{\epsilon}{2} - \sin^2 \varphi, \tag{18}$$

where 2φ denotes the angular deviation of the pendulum from the vertical, $\tau \equiv \nu t$ denotes the dimensionless time (with $\nu^2 \equiv g/L$ for a pendulum of length L in a gravitational field with acceleration magnitude g) and $\epsilon \equiv E/(MgL)$ denotes the normalized energy of the pendulum (of mass M).

We transform the differential equation (18) into the Jacobi differential equation (4) with the substitution $y(\tau) \equiv m^{-1/2} \sin \varphi$ (where $m \equiv \epsilon/2$) and thus the solution of the planar pendulum (for $m < 1$) is

$$\varphi(\tau) = \sin^{-1}[m^{1/2} \operatorname{sn}(\tau|m)]. \tag{19}$$

When $\epsilon > 2$ ($m > 1$), on the other hand, we use the identities (13) to obtain

$$\varphi(\tau) = \sin^{-1}[\operatorname{sn}(m^{1/2}\tau|m^{-1})]. \tag{20}$$

We note that the *libration* motion (19) of the planar pendulum has a period $4K(m)$ while the *rotation* motion (20) of the planar pendulum has a period $4m^{-1/2}K(m^{-1})$. In the limit $m = 1$, the identities (9) yield the *separatrix* solution

$$\varphi(\tau) = \sin^{-1}(\tanh \tau), \tag{21}$$

which is expressed in terms of singly periodic (hyperbolic) trigonometric functions (with an imaginary period). Since $\varphi \rightarrow \pi/2$ as $\tau \rightarrow \infty$, the period of the pendulum on the separatrix orbit is infinite.

Figure 6 shows the phase portrait (φ' versus φ) of the pendulum orbits (19)–(21). Here, for $m < 1$, the derivative of equation (19) yields the libration angular velocity

$$\varphi' = \frac{m^{1/2}}{\sqrt{1 - m \operatorname{sn}^2 \tau}} \operatorname{sn}' \tau = m^{1/2} \operatorname{cn}(\tau|m), \tag{22}$$

where the identities (7) and (8) are used. For $m > 1$, on the other hand, the rotation angular velocity is

$$\varphi' = m^{1/2} \operatorname{dn}(m^{1/2}\tau|m^{-1}), \tag{23}$$

where the identity (13) is used. Note that, since the rotation angular velocity (23) does not vanish (see figure 1), the rotation orbits in the phase portrait shown in figure 6 are generated with angular velocities of both signs. According to equation (9), the angular velocity on the separatrix orbit ($m = 1$) is $\varphi' = \operatorname{sech} \tau$, which implies that the pendulum's angular velocity approaches zero exponentially as the pendulum approaches $\varphi = \pi/2$. Each orbit in the phase portrait shown in figure 6 corresponds to the initial conditions $\varphi_0 = 0$ and $\varphi'_0 = \pm\sqrt{\epsilon/2}$ (only one sign is chosen for the libration orbits) and is generated with $-2K(\epsilon/2) < \tau < 2K(\epsilon/2)$ (for the libration orbits with $\epsilon < 2$) or $-2\sqrt{2/\epsilon}K(2/\epsilon) < \tau < 2\sqrt{2/\epsilon}K(2/\epsilon)$ (for the rotation orbits with $\epsilon > 2$). Note that the topology of the phase portrait for the planar pendulum is represented as a cylinder since the angle $\varphi = -\pi/2$ is physically identical to $\varphi = \pi/2$.

We shall return to the planar pendulum later in section 3.1 to highlight the connection between the Jacobi and Weierstrass elliptic functions (presented in appendix A).

2.3. Force-free asymmetric top

As a second physical example, we consider the Euler equations for a force-free asymmetric top (with principal moments of inertia $I_1 > I_2 > I_3$) [2]:

$$\left. \begin{aligned} I_1 \dot{\omega}_1 &= (I_2 - I_3)\omega_2\omega_3 \\ I_2 \dot{\omega}_2 &= -(I_1 - I_3)\omega_1\omega_3 \\ I_3 \dot{\omega}_3 &= (I_1 - I_2)\omega_1\omega_2 \end{aligned} \right\}, \quad (24)$$

where the angular velocity $\boldsymbol{\omega} = \omega_1 \hat{\mathbf{1}} + \omega_2 \hat{\mathbf{2}} + \omega_3 \hat{\mathbf{3}}$ is decomposed in terms of its components along the principal axes of inertia. The conservation laws of kinetic energy,

$$\kappa = \frac{1}{2}(I_1\omega_1^2 + I_2\omega_2^2 + I_3\omega_3^2) \equiv \frac{1}{2}I_0\Omega_0^2, \quad (25)$$

and (squared) angular momentum,

$$\ell^2 = I_1^2\omega_1^2 + I_2^2\omega_2^2 + I_3^2\omega_3^2 \equiv I_0^2\Omega_0^2, \quad (26)$$

are used to define the parameters $I_0 \equiv \ell^2/(2\kappa)$ and $\Omega_0 \equiv 2\kappa/\ell$. These parameters can be used to introduce the following definitions:

$$\begin{aligned} \omega_1(\tau) &= -\sqrt{\frac{I_0(I_0 - I_3)}{I_1(I_1 - I_3)}}\Omega_0\sqrt{1 - y^2(\tau)} \\ &\equiv -\Omega_1(I_0)\sqrt{1 - y^2(\tau)}, \end{aligned} \quad (27)$$

$$\begin{aligned} \omega_2(\tau) &= \sqrt{\frac{I_0(I_0 - I_3)}{I_2(I_2 - I_3)}}\Omega_0 y(\tau) \\ &\equiv \Omega_2(I_0)y(\tau), \end{aligned} \quad (28)$$

$$\begin{aligned} \omega_3(\tau) &= \sqrt{\frac{I_0(I_1 - I_0)}{I_3(I_1 - I_3)}}\Omega_0\sqrt{1 - my^2(\tau)} \\ &\equiv \Omega_3(I_0)\sqrt{1 - my^2(\tau)}, \end{aligned} \quad (29)$$

where $\tau = [(I_1 - I_3)\Omega_1\Omega_3/(I_2\Omega_2)]t$ is the dimensionless time used in equations (27)–(29) and the modulus m is defined as

$$m(I_0) \equiv \frac{(I_0 - I_3)(I_1 - I_2)}{(I_2 - I_3)(I_1 - I_0)}. \quad (30)$$

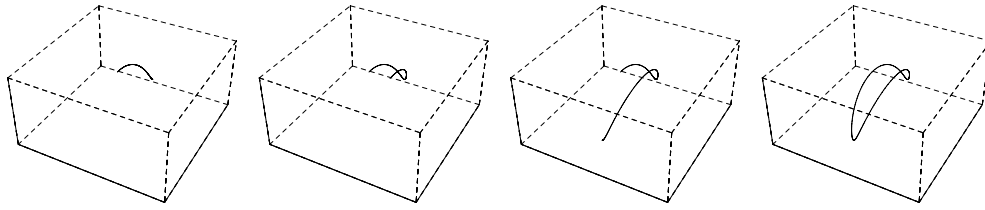


Figure 7. Three-dimensional $(\omega_1, \omega_2, \omega_3)$ plots of the orbit (31) for the asymmetric free top from $\tau = 0$ to (from left to right) $\tau = K(m)$, $\tau = 2K(m)$, $\tau = 3K(m)$ and $\tau = 4K(m)$.

By requiring that the modulus m be positive, the parameter $I_0 = \ell^2/2\kappa$ must satisfy $I_3 < I_0 < I_1$ and, hence, $0 \leq m(I_0) \leq 1$ for $I_3 \leq I_0 \leq I_2$ and $m(I_0) > 1$ for $I_2 < I_0 < I_1$ (with $m \rightarrow \infty$ as $I_0 \rightarrow I_1$).

When we substitute these expressions into the Euler equation (24) for $\omega_2 \equiv \Omega_2 y(\tau)$, we easily obtain the dimensionless Jacobi differential equation (4), which can now be integrated, with the initial conditions $(\omega_1(0), \omega_2(0), \omega_3(0)) = (-\Omega_1, 0, \Omega_3)$, to yield [2]

$$(\omega_1, \omega_2, \omega_3) = (-\Omega_1 \operatorname{cn} \tau, \Omega_2 \operatorname{sn} \tau, \Omega_3 \operatorname{dn} \tau), \tag{31}$$

whose orbit is shown in figure 7 where the $4K$ periodicity is clearly observed. The solution of this problem is thus very elegantly expressed in terms of the Jacobi elliptic functions (sn, cn, dn). Note also that the Jacobi identities (8) can be used to show that the solution (31) preserves the constants of the motion (25) and (26).

The separatrix solution ($m = 1$) corresponds to the case when $I_0 = I_2$ for which $\Omega_2 \equiv \Omega_0$, so that the separatrix solution is

$$\begin{aligned} \omega_1(\tau) &= -\sqrt{\frac{I_2(I_2 - I_3)}{I_1(I_1 - I_3)}} \Omega_0 \operatorname{sech} \tau, \\ \omega_2(\tau) &= \Omega_0 \tanh \tau, \\ \omega_3(\tau) &= \sqrt{\frac{I_2(I_1 - I_2)}{I_3(I_1 - I_3)}} \Omega_0 \operatorname{sech} \tau. \end{aligned}$$

Lastly, the motion of a symmetric top ($I_1 = I_2 \neq I_3$) corresponds to the limit $m \equiv 0$ (and $\Omega_2 = \Omega_1$). The Jacobian solution (31) for a symmetric top thus becomes $(\omega_1, \omega_2, \omega_3) = (-\Omega_1 \cos \tau, \Omega_1 \sin \tau, \Omega_3)$, where $\tau \equiv (1 - I_3/I_1)\Omega_3 t$ is now the dimensionless time.

3. Weierstrass elliptic functions

The Weierstrass elliptic function $\wp(z + \gamma) \equiv \wp(z + \gamma; g_2, g_3)$ is defined as the solution of the differential equation

$$\begin{aligned} \left(\frac{dy}{dz}\right)^2 &= 4y^3 - g_2y - g_3 \\ &\equiv 4(y - e_1)(y - e_2)(y - e_3), \end{aligned} \tag{32}$$

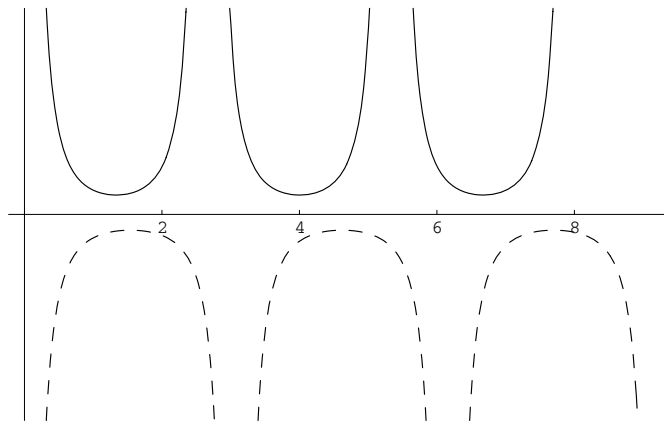


Figure 8. Plots of $\wp(z) > 0$ (solid lines) and $\wp(iz) < 0$ (dashed lines) for $g_2 = 3$ and $g_3 = 1/2$ (with $\Delta > 0$) showing the real period 2ω (upper graph) and the imaginary period $2\omega'$ (lower graph) defined, respectively, by equations (34) and (35).

Table 1. Cubic roots (e_1, e_2, e_3) and half-periods $(\omega_1, \omega_2, \omega_3)$ for the Weierstrass elliptic function.

(g_3, Δ)	e_1	e_2	e_3	ω_1	$\omega_2 \equiv \omega_1 + \omega_3$	ω_3
$(-, -)$	$a - ib$	$a + ib$	$-2a < -1$	$ \Omega' + i\Omega/2$	$ \Omega' - i\Omega/2$	$-i\Omega$
$(-, +)$	$d > 0$	$c - d > 0$	$-c < 0$	$ \omega' $	$-i\omega + \omega' $	$-i\omega$
$(+, +)$	$c > 0$	$d - c < 0$	$-d < 0$	ω	$\omega + \omega'$	ω'
$(+, -)$	$2a > 1$	$-a - ib$	$-a + ib$	Ω	$\Omega/2 + \Omega'$	$-\Omega/2 + \Omega'$

subject to the initial condition $y(0) = \wp(\gamma)$. Here, (e_1, e_2, e_3) denote the roots of the cubic polynomial $4y^3 - g_2y - g_3$ (such that $e_1 + e_2 + e_3 = 0$), and the invariants g_2 and g_3 are defined in terms of the cubic roots as [6, 8]

$$\left. \begin{aligned} g_2 &= -4(e_1e_2 + e_2e_3 + e_3e_1) \\ &= 2(e_1^2 + e_2^2 + e_3^2) \\ g_3 &= 4e_1e_2e_3 \end{aligned} \right\}. \tag{33}$$

The applications of Weierstrass elliptic functions are analysed in terms of four different cases (see table 1) based on the signs of $(g_3, \Delta) = [(-, -), (-, +), (+, -), (+, +)]$, where $\Delta = g_2^3 - 27g_3^2$ is the modular discriminant.

Figure 8 shows that, for $\Delta > 0$, $\wp(z)$ has different periods 2ω and $2\omega'$ along the real and imaginary axes, respectively, with the half-periods ω and ω' defined as

$$\omega(g_2, g_3) = \int_{e_1}^{\infty} \frac{ds}{\sqrt{4s^3 - g_2s - g_3}}, \tag{34}$$

$$\omega'(g_2, g_3) = i \int_{-\infty}^{e_3} \frac{ds}{\sqrt{|4s^3 - g_2s - g_3|}}. \tag{35}$$

Figure 9(a) shows the plots of $\omega(g_2, g_3)$ and $\omega'(g_2, g_3)$ for $g_2 = 3$ as functions of $0 < g_3 < 1$, with $\Delta = 27(1 - g_3^2) > 0$. Note that for $g_3 = 0$ (with $e_1 = -e_3$ and $e_2 = 0$), we find that $\omega' \equiv i\omega$ while $|\omega'|$ approaches infinity as g_3 approaches 1 (or Δ approaches zero). Explicit

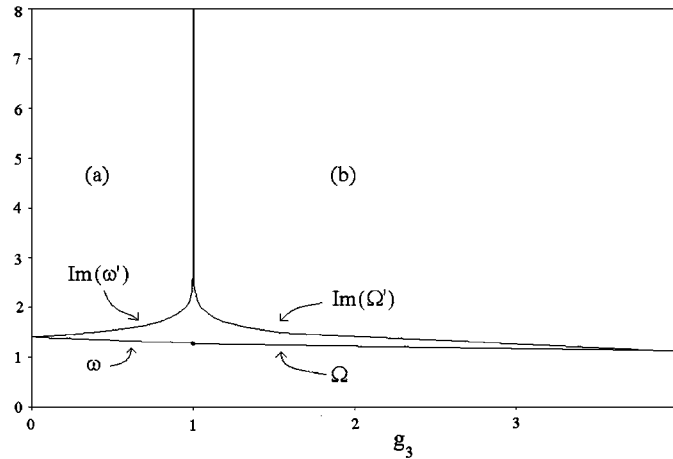


Figure 9. Plots of (a) ω and $\text{Im}(\omega')$ for $0 < g_3 < 1$ and $g_2 = 3$ (i.e., $\Delta > 0$) and (b) Ω and $\text{Im}(\Omega')$ for $g_3 > 1$ and $g_2 = 3$ (i.e., $\Delta < 0$). Note that, as $\Delta \rightarrow 0$ (i.e., $g_3 \rightarrow 1$ when $g_2 = 3$), both $\text{Im}(\omega')$ and $\text{Im}(\Omega')$ become infinite while $\Omega(g_2, 1) = \omega(g_2, 1)$. Lastly, $\omega'(g_2, 0) = i\omega(g_2, 0)$ and both (Ω, Ω') decrease to zero as g_3 becomes infinite.

calculations of the Weierstrass half-periods (34)–(35) in terms of Jacobian quarter-periods K and K' are given in appendix B.

For $\Delta < 0$, on the other hand, $\wp(z)$ has different periods 2Ω and $2\Omega'$ along the real and imaginary axes, respectively, with the half-periods Ω and Ω' defined as

$$\Omega(g_2, g_3) = \int_{e_1}^{\infty} \frac{ds}{\sqrt{4s^3 - g_2s - g_3}}, \tag{36}$$

$$\Omega'(g_2, g_3) = i \int_{-\infty}^{e_1} \frac{ds}{\sqrt{|4s^3 - g_2s - g_3|}}. \tag{37}$$

Figure 9(b) shows the plots of $\Omega(g_2, g_3)$ and $\Omega'(g_2, g_3)$ for $g_2 = 3$ as functions of $g_3 > 1$, with $\Delta = 27(1 - g_3^2) < 0$. Note that $\omega(g_2, 1) = \Omega(g_2, 1)$, $|\Omega'|$ approaches infinity as g_3 approaches 1, and that both Ω and Ω' approach zero as g_3 approaches infinity.

Table 1 shows the cubic roots $e_i = (e_1, e_2, e_3)$ and the half-periods $\omega_i = (\omega_1, \omega_2, \omega_3)$,¹ which satisfy the following definitions: [6] $\wp(\omega_i) \equiv e_i$ and $\wp(z + 2\omega_i) \equiv \wp(z)$, while, for $i \neq j \neq k$, we have the identity [6]

$$\wp(z + \omega_i) = e_i + \frac{(e_i - e_j)(e_i - e_k)}{\wp(z) - e_i}, \tag{38}$$

so that $\wp(\omega_i + \omega_j) = e_k$. Figure 10 shows the plots of $\wp(z + \omega_2)$ and $\wp(z + \omega_3)$ for one complete period from $z = 0$ to $2\omega_1$, which obey the identity (38). The singular behaviour predicted by equation (38) at $z = \omega_i$, on the other hand, is shown in figure 8 for $i = 1$ and $j, k \neq 1$. Additional properties of the Weierstrass elliptic function are that (i) it is an even-parity function $\wp(-z) = \wp(z)$, and (ii) under a change of sign $g_3 > 0 \rightarrow g_3 = -|g_3| < 0$ (with fixed g_2 and, thus, fixed discriminant Δ), the Weierstrass elliptic function satisfies the identity

$$\wp(z; g_2, g_3) \equiv -\wp(iz; g_2, |g_3|). \tag{39}$$

¹ The reader should be warned that only the case $(g_3, \Delta) = (+, +)$ follows the standard convention [8]. The convention presented in table 1 was developed from a careful study of particle orbits in a cubic potential [9].

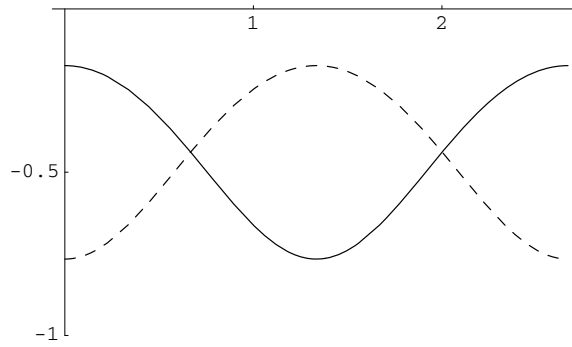


Figure 10. Plots of $\wp(z + \omega_2)$ (solid line) and $\wp(z + \omega_3)$ (dashed line) for $g_2 = 3$ and $g_3 = 1/2$ (with $\Delta > 0$) over one complete period from 0 to $2\omega_1$. Note that $\wp(\omega_j) = e_j$ for $j = 2$ or 3 and $\wp(\omega_i + \omega_j) = e_k$, for $i = 1$ and $(j, k) = (2, 3)$ or $(3, 2)$.

The g_3 -inversion identity (39) is used in table 1 for writing the following transformations $e_i^+(g_3 > 0) \rightarrow e_i^-(g_3 < 0)$ for the Weierstrass roots (for fixed g_2 and Δ):

$$\begin{pmatrix} e_1^- \\ e_2^- \\ e_3^- \end{pmatrix} \equiv \begin{pmatrix} \wp(\omega_1^-; g_2, g_3) \\ \wp(\omega_2^-; g_2, g_3) \\ \wp(\omega_3^-; g_2, g_3) \end{pmatrix} \equiv - \begin{pmatrix} \wp(i\omega_1^-; g_2, |g_3|) \\ \wp(i\omega_2^-; g_2, |g_3|) \\ \wp(i\omega_3^-; g_2, |g_3|) \end{pmatrix} \equiv - \begin{pmatrix} \wp(\omega_3^+; g_2, |g_3|) \\ \wp(\omega_2^+; g_2, |g_3|) \\ \wp(\omega_1^+; g_2, |g_3|) \end{pmatrix} \equiv - \begin{pmatrix} e_3^+ \\ e_2^+ \\ e_1^+ \end{pmatrix}, \tag{40}$$

which makes use of the transformation

$$(\omega_1^-, \omega_2^-, \omega_3^-) \equiv -i(\omega_3^+, \omega_2^+, \omega_1^+). \tag{41}$$

The transformations (40)–(41) were previously introduced in order to present a uniform solution of the problem of a particle moving in a cubic potential in terms of the Weierstrass elliptic function for all values of energy and for all bounded and unbounded orbits [9]. They also play a fundamental role in discussing the Weierstrass solution of the planar-pendulum problem (see equations (46) and (47)).

Lastly, we note that, in contrast to the simple rectangular form of the fundamental period–parallelogram of the Jacobi elliptic functions, the fundamental period–parallelogram $(0, \omega_1, \omega_2 = \omega_1 + \omega_3, \omega_3)$ of the Weierstrass elliptic function changes shape depending on the signs of (g_3, Δ) in table 1.

3.1. Planar pendulum

For our first example, we return to the planar-pendulum problem solved in section 2.2 in terms of the Jacobi elliptic functions. By writing $y = 2 \sin^2 \varphi$ (i.e., $0 < y < 2$), we transform equation (18) into the cubic-potential equation

$$(y')^2 = 2y(2 - y)(\epsilon - y), \tag{42}$$

with turning points at $y = 0, 2$ and ϵ . Physical motion is possible only when the right side of equation (42) is positive. Hence, the motion is periodic between $y = 0$ and $y = \epsilon$ for $\epsilon < 2$, while the motion is periodic between $y = 0$ and $y = 2$ for $\epsilon > 2$. We recover the standard Weierstrass differential equation (32) by setting

$$y(\tau) = 2\wp(\tau + \gamma) + \mu, \tag{43}$$

Table 2. Weierstrass roots (e_1, e_2, e_3) and Jacobi parameters $\kappa = \sqrt{e_1 - e_3}$ and $m = (e_2 - e_3)/(e_1 - e_3)$ for the planar-pendulum problem.

Case	(g_3, Δ)	ϵ	e_3	e_2	e_1	$\gamma = \omega_3$	Half-period ω_1	κ	m
(a)	(+, +)	$0 < \epsilon < 1$	$-\mu/2$	$\mu - 1$	$1 - \mu/2$	ω'	ω	1	$\epsilon/2$
(b)	(-, +)	$1 < \epsilon < 2$	$-\mu/2$	$\mu - 1$	$1 - \mu/2$	$-i\omega$	$ \omega' $	1	$\epsilon/2$
(c)	(-, +)	$2 < \epsilon < 4$	$-\mu/2$	$1 - \mu/2$	$\mu - 1$	$-i\omega$	$ \omega' $	$\sqrt{\epsilon/2}$	$2/\epsilon$
(d)	(+, +)	$4 < \epsilon$	$-\mu/2$	$1 - \mu/2$	$\mu - 1$	ω'	ω	$\sqrt{\epsilon/2}$	$2/\epsilon$

where $\mu \equiv (\epsilon + 2)/3$ and the constant γ is determined from the initial condition $y(0)$. The Weierstrass invariants g_2 and g_3 are

$$g_2 = 1 + 3(\mu - 1)^2 \quad \text{and} \quad g_3 = \mu(\mu - 1)(\mu - 2),$$

and the modular discriminant is $\Delta = \epsilon^2(2 - \epsilon)^2 \geq 0$.

The Weierstrass solution of the planar pendulum is discussed in terms of the four cases summarized in table 2, where the root $(-\mu/2)$ corresponds to the turning point $y = 0$, the root $(1 - \mu/2)$ corresponds to the turning point $y = 2$ and the root $(\mu - 1)$ corresponds to the turning point $y = \epsilon$. Using the initial conditions $y(0) = 0$ and $y'(0) = 0$, i.e., $\gamma \equiv \omega_3$ so that $\wp(\gamma) = e_3$, the Weierstrass solutions for cases (a) and (d) are expressed as

$$y(\tau) = 2\wp(\tau + \omega') + \mu, \tag{44}$$

where $\omega_3 = \omega'$ and the period of oscillation is $2\omega_1 = 2\omega$ (see $(g_3, \Delta) = (+, +)$ in table 1). For cases (b) and (c), the Weierstrass solutions are expressed as

$$y(\tau) = 2\wp(\tau - i\omega) + \mu, \tag{45}$$

where $\omega_3 = -i\omega$ and the period of oscillation is the period of oscillation $2\omega_1 = 2|\omega'|$ (see $(g_3, \Delta) = (-, +)$ in table 1). As expected, when $\epsilon \rightarrow 2$ (i.e., $\Delta \rightarrow 0$), the period $2|\omega'|$ approaches infinity as we approach the pendulum's separatrix (see figure 9).

Each pair of cases (a)–(b) and (c)–(d) in table 2 satisfies the transformations (40)–(41). Consider, for example, the pair (a)–(b): in case (a), we denote the initial angle as φ_0 (with $\varphi'_0 = 0$), where $0 < \varphi_0 < \pi/4$, so that $0 < \epsilon = 2 \sin^2 \varphi_0 < 1$, while in case (b), we denote the initial angle as $\bar{\varphi}_0$ (with $\bar{\varphi}'_0 = 0$), where $\pi/4 < \bar{\varphi}_0 < \pi/2$, so that $1 < \bar{\epsilon} \equiv 2 \sin^2 \bar{\varphi}_0 < 2$. We now introduce the transformation

$$\begin{pmatrix} \varphi_0 \\ \epsilon \end{pmatrix} \rightarrow \begin{pmatrix} \bar{\varphi}_0 \\ \bar{\epsilon} \end{pmatrix} \equiv \begin{pmatrix} \pi/2 - \varphi_0 \\ 2 - \epsilon \end{pmatrix}, \tag{46}$$

which generates the g_3 -inversion transformation $(g_2, g_3, \Delta) \rightarrow (\bar{g}_2, \bar{g}_3, \bar{\Delta}) = (g_2, -g_3, \Delta)$ on the Weierstrass invariants for the planar pendulum. From the transformation (46), we obtain $\mu \rightarrow \bar{\mu} = 2 - \mu$, and thus $(e_1, e_2, e_3) \rightarrow (\bar{e}_1, \bar{e}_2, \bar{e}_3) = -(e_3, e_2, e_1)$ and $(\omega_1, \omega_2, \omega_3) \rightarrow (\bar{\omega}_1, \bar{\omega}_2, \bar{\omega}_3) = -i(\omega_3, \omega_2, \omega_1)$, in exact agreement with the transformations (40)–(41). Next, the solution $\bar{y}(\tau; \bar{\omega}_1) = 2\wp(\tau + \bar{\omega}_3; \bar{g}_2, \bar{g}_3) + \bar{\mu}$, which has the real half-period $\bar{\omega}_1 = |\omega'|$, is expressed as

$$\begin{aligned} \bar{y}(\tau; \bar{\omega}_1) &= 2\wp(\tau - i\omega_1; g_2, -g_3) + (2 - \mu) \\ &= 2 - (2\wp(i\tau + \omega_1; g_2, g_3) + \mu) \equiv 2 - y(i\tau; -i\omega_3), \end{aligned} \tag{47}$$

where the solution $y(i\tau; -i\omega_3)$, which has the real half-period $-i\omega_3 = |\omega'|$, is a function of *imaginary* time $i\tau$. Because the normalized time $\tau \equiv (g/L)^{1/2}t$ involves the gravitational acceleration g , we obtain an imaginary time if we invert gravity's direction ($g \rightarrow \bar{g} \equiv -g$), so that $\tau \rightarrow \bar{\tau} \equiv i\tau$ and $y(i\tau; -i\omega_3) \equiv y(\bar{\tau}; |\omega'|)$. The physical interpretation of the imaginary

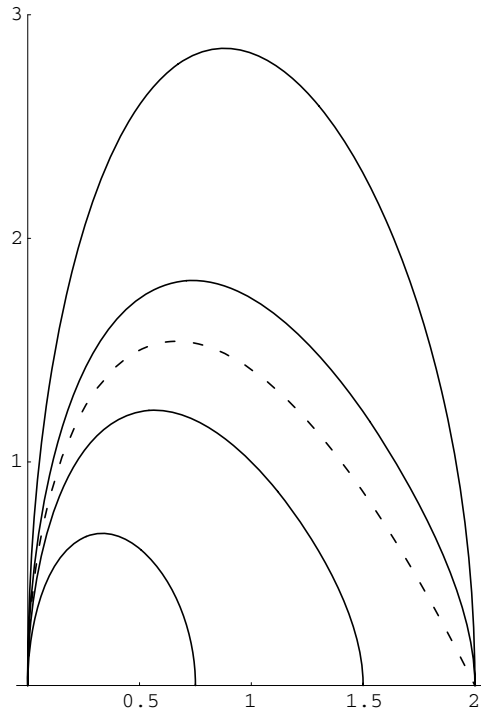


Figure 11. Upper half of the phase portrait (y' versus y) for the planar pendulum represented in terms of the Weierstrass elliptic solutions (44) and (45). The separatrix orbit (dashed curve with $\epsilon = 2$) separates the libration orbits (a) and (b) (inner curves with turning points 0 and $\epsilon < 2$) from the rotation orbits (c) and (d) (outer curves with turning points 0 and 2).

half-period ω' of the planar pendulum is, therefore, that its magnitude $|\omega'|$ is the real half-period of the inverted planar pendulum (or pendulum with imaginary time) [1].

Figure 11 shows the phase portrait ($y' = 2\wp'$ versus $y = 2\wp + \mu$) for the planar pendulum represented in terms of the Weierstrass elliptic solutions (44) and (45). Here, the orbits are labelled with $\epsilon = (0.75, 1.5, 2, 2.5, 5)$, from the inner curve ($\epsilon = 0.75$) to the outer curve ($\epsilon = 5$), and each orbit is generated with $-\omega_1 < \tau < \omega_1$. We note that the transformation $y = 2 \sin^2 \varphi$ has replaced the Jacobian phase portrait (figure 6), whose nontrivial topology is represented as an infinite cylinder, with the Weierstrassian phase portrait (figure 11), whose trivial topology is represented as an infinite strip (because y is limited to the range $0 \leq y \leq 2$ and $-\infty < y' < \infty$).

Lastly, the solution of the planar pendulum in terms of the Jacobi elliptic function $\text{sn}(z|m)$ and the Weierstrass elliptic function $\wp(z+\gamma)$ suggests a close connection between these elliptic functions. A derivation of the relations between the Jacobi and Weierstrass elliptic functions is presented in appendix A (see equations (A.5)–(A.7)). Using equation (A.6), for example, we indeed find the general solution for the planar pendulum for all values of normalized energy ϵ :

$$2\wp(\tau + \omega_3) + \mu = 2m\kappa^2 \text{sn}^2(\kappa\tau|m) = \begin{cases} \epsilon \text{sn}^2(\tau|\epsilon/2) & (\epsilon < 2) \\ 2 \text{sn}^2(\sqrt{\epsilon/2}\tau|2/\epsilon) & (\epsilon > 2) \end{cases}, \quad (48)$$

where $\kappa = \sqrt{e_1 - e_3}$ and $m = (e_2 - e_3)/(e_1 - e_3)$ (see table 2). Appendix B shows that the Weierstrass half-periods ω and ω' are related to the Jacobian quarter-periods K and K' as $\omega \equiv K(m)$ and $\omega' = iK'$.

3.2. Spherical pendulum

Our second example is the spherical pendulum (whose pendulum bob moves on the surface of a unit sphere), which is described here in terms of the cylindrical coordinates (ρ, φ, z) [1]. The energy equation for a spherical pendulum of unit mass and unit length is

$$\epsilon v^2 = \frac{1}{2}(\dot{\rho}^2 + \rho^2 \dot{\varphi}^2 + \dot{z}^2) + v^2 z,$$

where ϵ denotes the normalized total energy ($v^2 \equiv g$). By substituting $\rho(z) = \sqrt{1 - z^2}$ (where $-1 \leq z \leq 1$) and the angular momentum conservation law $\ell \equiv \rho^2 \dot{\varphi}/v$, we obtain the differential equation

$$\begin{aligned} (z')^2 &= 2(\epsilon - z)(1 - z^2) - \ell^2 \\ &\equiv 2(z - z_1)(z - z_2)(z - z_3), \end{aligned} \tag{49}$$

where $z'(\tau) \equiv v^{-1} \dot{z}$ and $z_1 + z_2 + z_3 = \epsilon$. Because the right side of equation (49) is negative at $z = \pm 1$, the highest root $z_1 (> 1 > z_2 > z_3 > -1)$ of the cubic polynomial is unphysical (since the cylindrical radius ρ then becomes imaginary). The periodic motion of the spherical pendulum is therefore bounded between $z_3 < z < z_2$.

The differential equation (49) can be transformed into the standard differential equation (32) by setting $z(\tau) = 2\wp(\tau + \gamma) + \mu$, where $\mu \equiv \epsilon/3$, the constant γ is determined from the initial condition $z(0)$, and the invariants g_2 and g_3 are $g_2 = 1 + 3\mu^2$ and $g_3 = \ell^2/4 + \mu(\mu^2 - 1)$. If we choose the initial condition $z(0) = z_3 > -1$, then the constant γ is $\gamma = \omega_3 = \omega'$ and the solution of the spherical pendulum problem for the z (and ρ) coordinate is

$$z(\tau) = 2\wp(\tau + \omega_3) + \mu \equiv \sqrt{1 - \rho^2(\tau)}. \tag{50}$$

The motion is periodic with half-period $\omega_1 = \omega$ so that $z(\omega_1) = 2\wp(\omega_1 + \omega_3) + \mu = 2\wp(\omega_2) + \mu \equiv z_2 < 1$ as expected. Note that we recover the planar pendulum (discussed in section 3.1) as a special case of the spherical pendulum with $\ell \equiv 0$ and a suitable change of definition for (z, ϵ, μ) .

The solution for the azimuthal angle $\varphi(\tau)$ is obtained from the angular-momentum conservation law $\varphi'(\tau) = \ell/\rho^2(\tau)$, which is integrated as [1]

$$\begin{aligned} \varphi(\tau) &= \ell \int_0^\tau \frac{ds}{1 - [2\wp(s + \omega_3) + \mu]^2} \\ &\equiv -\frac{\ell}{4} \int_0^\tau \frac{ds}{[\wp(s + \omega_3) - \wp(\kappa)][\wp(s + \omega_3) - \wp(\lambda)]}, \end{aligned} \tag{51}$$

where we used the initial condition $\varphi(0) = 0$ and the imaginary constants κ and λ are defined by the relations $\wp(\kappa) = -(1 + \mu)/2$ and $\wp(\lambda) = (1 - \mu)/2$ corresponding to $z = -1 < z_3$ and $z = +1 > z_2$, respectively. These constants also yield the relations $\wp'(\kappa) = i\ell/2 = \wp'(\lambda)$, obtained from the Weierstrass differential equation (32) for $z = \kappa$ and λ . These relations allow us to write equation (51) as

$$\varphi(\tau) = \frac{i}{2} \int_0^\tau ds \left[\frac{\wp'(\lambda)}{\wp(s + \omega_3) - \wp(\lambda)} - \frac{\wp'(\kappa)}{\wp(s + \omega_3) - \wp(\kappa)} \right], \tag{52}$$

where we used the identity $\wp(\lambda) - \wp(\kappa) = 1$.

The integral (52) can be solved exactly in terms of the quasi-periodic functions $\zeta(\tau)$ and $\sigma(\tau)$ associated with the Weierstrass elliptic function $\wp(\tau)$ [6]: $\wp(\tau) \equiv -d\zeta(\tau)/d\tau$ and $\zeta(\tau) \equiv \sigma'(\tau)/\sigma(\tau)$. Using the identity

$$\begin{aligned} \frac{\wp'(\lambda)}{\wp(s) - \wp(\lambda)} &\equiv \zeta(s - \lambda) - \zeta(s + \lambda) + 2\zeta(\lambda) \\ &= \frac{d}{ds} \ln \left(\frac{\sigma(s - \lambda)}{\sigma(s + \lambda)} \right) + 2\zeta(\lambda), \end{aligned}$$

we find the standard solution [1] for the azimuthal motion of the spherical pendulum

$$e^{2i\varphi(\tau)} = e^{2\tau[\zeta(\kappa) - \zeta(\lambda)]} \left[\left(\frac{\sigma(\tau + \omega_3 + \lambda)\sigma(\omega_3 - \lambda)}{\sigma(\omega_3 + \lambda)\sigma(\tau + \omega_3 - \lambda)} \right) \times \left(\frac{\sigma(\tau + \omega_3 - \kappa)\sigma(\omega_3 + \kappa)}{\sigma(\omega_3 - \kappa)\sigma(\tau + \omega_3 + \kappa)} \right) \right], \quad (53)$$

where we can easily verify that $\varphi(0) = 0$. This solution (presented in Whittaker's book [1]) can be studied numerically with Mathematica since its library of functions contains the Weierstrass elliptic function $\wp(\tau)$ and its associated quasi-periodic functions $\zeta(\tau)$ and $\sigma(\tau)$.

It turns out that we may further simplify the standard solution (53) by recognizing that, since $-1 < z_3 \leq \wp(\tau + \omega_3) \leq z_2 < +1$ for real values of τ , there must be imaginary numbers $i\alpha$ and $i\beta$ (where α and β are real-valued constants) such that $\kappa \equiv \omega_3 + i\alpha$ and $\lambda \equiv \omega_3 + i\beta$. Using these substitutions, the solution (53) becomes

$$e^{2i\varphi(\tau)} = e^{2\tau[\zeta(\kappa) - \zeta(\lambda)]} \left[\left(\frac{\sigma(\tau + 2\omega_3 + i\beta)\sigma(-i\beta)}{\sigma(2\omega_3 + i\beta)\sigma(\tau - i\beta)} \right) \times \left(\frac{\sigma(\tau - i\alpha)\sigma(2\omega_3 + i\alpha)}{\sigma(-i\alpha)\sigma(\tau + 2\omega_3 + i\alpha)} \right) \right]. \quad (54)$$

Next, using the identity [6] $\sigma(\tau + 2\omega_3) \equiv -\exp[2\eta_3(\tau + \omega_3)]\sigma(\tau)$, where $\eta_3 \equiv \zeta(\omega_3)$, we now find

$$\frac{\sigma(\tau + 2\omega_3 + i\beta)}{\sigma(\tau - i\beta)} = -e^{2\eta_3(\tau + i\beta)} \frac{\sigma(\tau + i\beta)}{\sigma(\tau - i\beta)}$$

and

$$\frac{\sigma(-i\beta)}{\sigma(2\omega_3 + i\beta)} = -e^{-2i\eta_3\beta} \frac{\sigma(-i\beta)}{\sigma(i\beta)} \equiv e^{-2i\eta_3\beta},$$

where we used the fact that $\sigma(\tau)$ is an odd function of τ , so that $\sigma(-i\beta) = -\sigma(i\beta)$. Hence, we obtain

$$\frac{\sigma(\tau + 2\omega_3 + i\beta)\sigma(-i\beta)}{\sigma(2\omega_3 + i\beta)\sigma(\tau - i\beta)} \equiv -e^{2\eta_3\tau} \left[\frac{\sigma(\tau + i\beta)}{\sigma(\tau - i\beta)} \right],$$

and

$$\frac{\sigma(\tau - i\alpha)\sigma(2\omega_3 + i\alpha)}{\sigma(-i\alpha)\sigma(\tau + 2\omega_3 + i\alpha)} \equiv -e^{-2\eta_3\tau} \left[\frac{\sigma(\tau - i\alpha)}{\sigma(\tau + i\alpha)} \right].$$

We combine these relations to obtain the simplified solution

$$e^{2i\varphi(\tau)} \equiv e^{2\tau[\zeta(\kappa) - \zeta(\lambda)]} \left[\frac{\sigma(\tau + i\beta)\sigma(\tau - i\alpha)}{\sigma(\tau - i\beta)\sigma(\tau + i\alpha)} \right]. \quad (55)$$

Lastly, we note that the ratio $\sigma(\tau + i\beta)/\sigma(\tau - i\beta)$ must have unit modulus for real τ -values, so that we may write

$$\begin{aligned} \ln \left(\frac{\sigma(\tau + i\beta)}{\sigma(\tau - i\beta)} \right) &= i \int_{-\beta}^{\beta} \zeta(\tau + is) ds \\ &= 2i \int_0^{\beta} \operatorname{Re}[\zeta(\tau + is)] ds. \end{aligned}$$

Hence, the solution (53) for the azimuthal angle $\varphi(\tau)$ can finally be given in a more compact form as

$$\begin{aligned} \varphi(\tau) &= \int_{\alpha}^{\beta} \operatorname{Re}[\zeta(\tau + is)] ds + i\tau[\zeta(\omega_3 + i\beta) - \zeta(\omega_3 + i\alpha)] \\ &\equiv \operatorname{Re} \left(\int_{\alpha}^{\beta} [\zeta(\tau + is) + \tau \wp(\omega_3 + is)] ds \right), \end{aligned} \tag{56}$$

which is now expressed only in terms of the quasi-periodic function $\zeta(\tau)$ and $\wp(\tau) = -\zeta'(\tau)$. After a full period $2\omega_1$, when the (ρ, z) -coordinates return to their initial values, the azimuthal angle has changed by an amount $\Delta\varphi \equiv \varphi(\tau + 2\omega_1) - \varphi(\tau)$ expressed as

$$\Delta\varphi = 2\omega_1 \int_{\alpha}^{\beta} \wp(\omega_3 + is) ds + 2\eta_1(\beta - \alpha), \tag{57}$$

where we used the identity [6] $\zeta(\tau + 2\omega_1 + is) = \zeta(\tau + is) + 2\eta_1$ and $\eta_1 \equiv \zeta(\omega_1)$.

The problem of the spherical pendulum, expressed in terms of the cylindrical coordinates (ρ, φ, z) , is thus exactly (and compactly) solved by equations (50) and (56) in terms of the Weierstrass elliptic function $\wp(\tau + \gamma)$ and its associated function $\zeta(\tau)$.

3.3. Heavy symmetric top with one fixed point

Our final example is provided by the motion of a symmetric top ($I_1 = I_2 \neq I_3$) with one fixed point described in terms of the energy equation

$$E = \frac{1}{2} \left[I_1 \dot{\theta}^2 + I_3 \varpi_3^2 + \frac{(p_{\varphi} - p_{\psi} \cos \theta)^2}{I_1 \sin^2 \theta} \right] + Mgh \cos \theta,$$

where E is the total energy of the symmetric top (with total mass M and principal moments of inertial $I_1 = I_2 \neq I_3$), ϖ_3 denotes the constant component of the angular velocity and the angular momenta p_{φ} and p_{ψ} associated with the ignorable Eulerian angles φ and ψ are constants of motion. By defining the dimensionless parameters $\epsilon = (E - \frac{1}{2} I_3 \varpi_3^2) / (Mgh)$, $(a, b) = (p_{\varphi} / I_1 v, p_{\psi} / I_1 v)$, where $v^2 = Mgh / (2I_1)$, the differential equation for $u = \cos \theta$ is obtained from equation (58) as

$$\begin{aligned} (u')^2 &= 4(1 - u^2)(\epsilon - u) - (a - bu)^2 \\ &\equiv 4(u - u_1)(u - u_2)(u - u_3), \end{aligned} \tag{59}$$

where the prime denotes a derivative with respect to the dimensionless time $\tau = vt$ and $u_3 < u_2 < u_1$ are the three roots of the cubic polynomial on the right side of equation (59). Since the right side of equation (59) is negative at $u = \pm 1$, we conclude that $-1 < u_3 < u_2 < 1$ and $u_1 > 1$ (which is unphysical for $u = \cos \theta$). The physical motion is therefore periodic in θ and is bounded between $u_3 \equiv \cos \theta_3$ and $u_2 \equiv \cos \theta_2$ (or $\theta_2 < \theta(\tau) < \theta_3$).

By using the change of integration variable $u = \wp + \mu$, where $\mu = (4\epsilon + b^2) / 12$, the differential equation (59) becomes the standard differential equation (32) for the Weierstrass elliptic function, where the invariants

$$\left. \begin{aligned} g_2 &= 2(2 - ab + 6\mu^2) \\ g_3 &= (a^2 + b^2) + 2\mu(4\mu^2 - 4 - ab) \end{aligned} \right\} \tag{60}$$

and the discriminant $\Delta = g_2^3 - 27g_3^2$ depend on the three constants of the motion (ϵ, a, b) for the problem. Hence, the solution is expressed in terms of the Weierstrass elliptic function as

$$u(\tau) \equiv \cos \theta(\tau) = \wp(\tau + \gamma) + \mu, \tag{61}$$

where γ is determined from the initial condition $\theta(0)$. Assuming that $-1 < u_3 = e_3 + \mu < u_2 = e_2 + \mu < 1 < u_1 = e_1 + \mu$, we choose $u(0) = e_3 + \mu = u_3$ (i.e., $-1 - \mu < e_3 < 1 - \mu$) so that $\gamma \equiv \omega'$ and, hence, at the half-period $\tau = \omega$, we find $u(\omega) = \wp(\omega + \omega') + \mu = e_2 + \mu = u_2$ as expected.

The solution (61) for the Eulerian angle $\theta(\tau)$ can now be used to integrate the differential equations for the remaining Euler angles φ and ψ :

$$\begin{aligned} \varphi'(\tau) &= \frac{a - b \cos \theta(\tau)}{1 - \cos^2 \theta(\tau)} \\ &\equiv \frac{i}{2} \left[\frac{\wp'(\kappa)}{\wp(\tau + \omega_3) - \wp(\kappa)} - \frac{\wp'(\lambda)}{\wp(\tau + \omega_3) - \wp(\lambda)} \right], \end{aligned} \quad (62)$$

and, defining $\psi' \equiv (\omega_3/v - b) + \chi'$,

$$\begin{aligned} \chi'(\tau) &= \frac{b - a \cos \theta(\tau)}{1 - \cos^2 \theta(\tau)} \\ &\equiv \frac{i}{2} \left[\frac{\wp'(-\kappa)}{\wp(\tau + \omega_3) - \wp(-\kappa)} - \frac{\wp'(\lambda)}{\wp(\tau + \omega_3) - \wp(\lambda)} \right], \end{aligned} \quad (63)$$

where $\wp(\kappa) = 1 - \mu$ and $\wp(\lambda) = -(1 + \mu)$, with $\wp'(\kappa) = i(a - b)$ and $\wp'(\lambda) = i(a + b)$. Note that the sign of φ' in equation (62) depends on the sign of $a - b \cos \theta_2 < a - b \cos \theta < a - b \cos \theta_3$. If $a > b \cos \theta_2$ (or $a < b \cos \theta_3$), φ' does not change sign as θ bounces between θ_2 and θ_3 and the motion in φ involves monotonic azimuthal precession. If $a = b \cos \theta_2$ (or $a = b \cos \theta_3$), φ' vanishes at $\theta = \theta_2$ (or $\theta = \theta_3$) and the motion in φ exhibits a cusp at that angle (since both θ' and φ' vanish). If $a < b \cos \theta_2$, φ' vanishes at an angle $\theta_2 < \theta_0 < \theta_3$ and the motion in φ exhibits retrograde motion between $\theta_0 < \theta < \theta_3$.

Lastly, since equation (62) is the same as equation (52), its solution is identical to equation (56) (even if the constants κ and λ are different). This same solution can also be applied to the solution for equation (63), where equation (62) is transformed into equation (63) by performing the change $(a, b) \rightarrow (b, a)$ and noting that $\wp(\tau)$ has even parity, i.e., $\wp(-\kappa) = \wp(\kappa)$, while $\wp'(\tau)$ has odd parity, i.e., $\wp'(-\kappa) = -\wp'(\kappa)$.

4. Other applications of elliptic functions in physics

The previous two sections showed problems of classical mechanics, involving the orbital motions of particles and rigid bodies, that can be solved explicitly in terms of Jacobi and Weierstrass elliptic functions. More problems of classical mechanics with solutions expressed in terms of the Jacobi and Weierstrass elliptic functions can be found in Whittaker's textbook [1] as well as more recent textbooks [9, 11]. These special functions have many more applications outside of classical mechanics as well [11], including particle orbits and light paths in general relativity [12] and solutions of cosmological models [13]. These applications unfortunately involve advanced topics that fall well outside the purpose of the present work.

One interesting application worthy of discussion, however, deals with exact solutions of the Korteweg–de Vries (KdV) equation [14]

$$\frac{\partial u}{\partial t} + u \frac{\partial u}{\partial x} + \frac{\partial^3 u}{\partial x^3} = 0, \quad (64)$$

which describes the nonlinear evolution of the field $u(x, t)$. This nonlinear equation appears in many areas of physics [15] and is a member of an important class of nonlinear partial differential equations that possesses soliton solutions [16–18].

A travelling-wave solution of the Korteweg–de Vries (KdV) equation (64) is a function of the form $u(x, t) = v(\xi)$, where $\xi = \kappa(x - ct)$ denotes the wave phase (with constants κ and

c to be determined). Substituting this travelling solution into the KdV equation, we obtain an ordinary differential equation for $v(\xi)$:

$$(v - c)v' + \kappa^2 v''' = 0,$$

which can be integrated with respect to ξ to yield

$$\kappa^2 v'' = \alpha + cv - \frac{1}{2}v^2, \quad (65)$$

where α is a constant of integration. If we multiply equation (65) with v' and integrate again with respect to ξ , we obtain

$$\frac{\kappa^2}{2}(v')^2 = (\alpha v + \beta) + \frac{c}{2}v^2 - \frac{1}{6}v^3, \quad (66)$$

where β is a second constant of integration. It is now immediately clear that $v(\xi) \equiv A\wp(\xi) + B$ can be expressed in terms of elliptic functions (where $A \equiv -12\kappa^2$, $B \equiv c$) because the right side of equation (66) involves a cubic polynomial in v . The travelling-wave solution of the KdV equation (64) is

$$u(x, t) = A\wp[\kappa(x - ct) + \gamma] + B,$$

where the constant γ is determined from the initial condition $u(x, 0) = u_0(x)$.

Using the relation between the Weierstrass and Jacobi elliptic functions (see appendix A), the travelling-wave solution to the KdV equation (64) may also be expressed as [17, 19]

$$u(x, t) = a \operatorname{cn}^2[\kappa(x - ct) + \gamma|m] + b,$$

where $m = \sqrt{(r_3 - r_2)/(r_3 - r_1)}$, $a = r_3 - r_2$, $b = r_2$ and $\kappa = \sqrt{(r_3 - r_1)/6}$; here, $r_1 < r_2 < r_3$ are the roots of the cubic polynomial on the right side of equation (66). This second representation is known as the periodic *cnoidal*-wave solution of the KdV equation (64).

Lastly, we note that for the special case $\alpha = 0 = \beta$ in equation (66), for which $r_3 = 3c$ and $r_1 = 0 = r_2$, then we find $m = 1$, $a = 3c$, $b = 0$, $\kappa = \sqrt{c/2}$, and the travelling-wave solution becomes

$$u(x, t) = 3c \operatorname{sech}^2 \left[\sqrt{\frac{c}{2}}(x - ct) \right],$$

which describes the well-known localized soliton solution of the KdV equation (64).

5. Summary

We presented a brief introduction of the Jacobi and Weierstrass elliptic functions with applications in classical mechanics. The problem of the planar pendulum was used to establish a connection (equation (48)) between the Jacobi and Weierstrass elliptic functions. The double periodicity of the elliptic functions was easily observed in each of the problems of classical mechanics discussed in sections 2 and 3. We also briefly discussed applications of the elliptic functions in section 4 in other areas of physics (e.g., travelling-wave solutions of the Korteweg–de Vries equation).

Because of their similarity with trigonometric functions $\sin z$ and $\cos z$, physicists are most familiar with the Jacobi elliptic functions $\operatorname{sn}(z|m)$ and $\operatorname{cn}(z|m)$. This familiarity is further increased by the fact that the problems of the planar pendulum and the force-free asymmetric top are solved simply and elegantly in terms of the Jacobi elliptic functions (as shown in section 2).

Physicists are usually less familiar with the Weierstrass elliptic function $\wp(z; g_2, g_3)$, introduced in section 3. The complexity of the Weierstrass elliptic function is partly due to

the fact that the form of its fundamental period–parallelogram depends on the invariants g_2 and g_3 (and the modular discriminant $\Delta = g_2^3 - 27g_3^2$). This is in contrast to the fundamental period–parallelogram of the Jacobi elliptic function which remains rectangular for all values of $m \neq 1$. The greatest advantage of the Weierstrass elliptic function, however, is that the function $\wp(z)$ itself and its derivative $\wp'(z)$ can be used to represent any doubly periodic function $f(z) \equiv A(\wp)\wp' + B(\wp)$, where A and B are arbitrary functions. This simplicity was further demonstrated by the solution of the planar pendulum in terms of a single expression (48) for all values of energy.

While the introduction of the Jacobi and Weierstrass elliptic functions in the undergraduate curriculum remains difficult, it is hoped that the present primer, combined with the easy access to mathematical software, will facilitate their dissemination.

Appendix A. Relation between Weierstrass and Jacobi elliptic functions

In this appendix, we explore the connection between the Jacobi and Weierstrass elliptic functions. For this purpose, we begin with the differential equation for the Weierstrass elliptic function

$$\left(\frac{dy}{dx}\right)^2 = 4y^3 - g_2y - g_3, \quad (\text{A.1})$$

and introduce the transformation

$$y(x) = \alpha s^p(\kappa x) + \beta, \quad (\text{A.2})$$

where p is an integer ($\neq 0, 1$) and (α, β, κ) are constants to be determined. Under the transformation (A.2), equation (A.1) becomes (with $z = \kappa x$)

$$\left(\frac{ds}{dz}\right)^2 = \frac{4\alpha}{p^2\kappa^2}s^{2+p} + \frac{12\beta}{p^2\kappa^2}s^2 + (12\beta^2 - g_2)\frac{s^{2-p}}{\alpha p^2\kappa^2} + (4\beta^3 - g_2\beta - g_3)\frac{s^{2-2p}}{\alpha^2 p^2\kappa^2}. \quad (\text{A.3})$$

The constants (α, β, κ) and the integer $p \neq 0, 1$ are chosen such that the right side of equation (A.3) has the Jacobi form (4). For $p = 2$, we recover the Jacobi form (4) if

$$\beta = -(m+1)\frac{\kappa^2}{3} \quad (\text{A.4})$$

is a root of the cubic polynomial $4\beta^3 - g_2\beta - g_3$ (i.e., $\beta = e_1, e_2$, or e_3) and

$$\alpha = m\kappa^2 = \frac{12\beta^2 - g_2}{4\kappa^2}.$$

For $p = -2$, on the other hand, we recover the Jacobi form (4) if β , given by equation (A.4), is again a root of the cubic polynomial $4\beta^3 - g_2\beta - g_3$ (i.e., $\beta = e_1, e_2$, or e_3) and

$$\alpha = \kappa^2 = \frac{12\beta^2 - g_2}{4m\kappa^2}.$$

Hence, the Jacobi elliptic function $s(z)$ is related to the Weierstrass elliptic function $y(x)$ in the case of $p = \pm 2$.

An application of the first transformation ($p = 2$) shows that for $m = (e_2 - e_3)/(e_1 - e_3)$ and $\kappa = \sqrt{e_1 - e_3}$, we find $\alpha = e_2 - e_3$ and $\beta = e_3$, and we obtain the relation

$$\wp(x + \omega_2; g_2, g_3) = e_3 + (e_2 - e_3)\text{cn}^2(\kappa x|m) \quad (\text{A.5})$$

or

$$\wp(x + \omega_3; g_2, g_3) = e_3 + (e_2 - e_3)\text{sn}^2(\kappa x|m), \quad (\text{A.6})$$

which oscillates between $e_2 = \wp(\omega_2) = \wp(\omega + \omega_3)$ and $e_3 = \wp(\omega + \omega_2) = \wp(\omega_3)$ (see figure 10), where $\omega = K(m)/\kappa$. Relation (A.6) plays a crucial role in expressing the Weierstrassian solution of the planar pendulum in terms of its Jacobian solution in equation (48).

An application of the second transformation ($p = -2$) shows that for the same m and κ as the first transformation, we find $\alpha = e_1 - e_3$ and $\beta = e_3$, and we obtain the relation

$$\wp(x; g_2, g_3) = e_3 + \frac{e_1 - e_3}{\text{sn}^2(\kappa x|m)}, \tag{A.7}$$

which has singularities at $x = 0$ and $2K(m)/\kappa \equiv 2\omega$ and a minimum (e_1) at $x = K(m)/\kappa \equiv \omega$ (see the upper plot in figure 8). We note that the relation (A.7) is equivalent to the property (38) of the Weierstrass elliptic function:

$$\wp(x) = e_3 + \frac{(e_1 - e_3)(e_2 - e_3)}{\wp(x + \omega_3) - e_3},$$

when substituting equation (A.6) into the denominator of equation (A.7).

Appendix B. Mathematical details

In this appendix, where we assume $(g_3, \Delta) = (+, +)$, we show how the half-periods ω and ω' of the Weierstrass elliptic function, defined in equations (34) and (35), are related to the quarter periods K and K' of the Jacobi elliptic function.

First, we start with the half-period (34). By introducing the change of variable [20] $s = e_3 + (e_1 - e_3) \text{csc}^2 \psi$, equation (34) transforms into

$$\begin{aligned} \omega(g_2, g_3) &= \int_0^{\pi/2} \frac{d\psi}{\sqrt{(e_1 - e_3) - (e_2 - e_3) \sin^2 \psi}} \\ &\equiv \frac{K(m)}{\sqrt{e_1 - e_3}}, \end{aligned} \tag{B.1}$$

where the modulus m of the Jacobian quarter period is defined by the relation $m = (e_2 - e_3)/(e_1 - e_3)$.

Next, we look at the half-period (35). By introducing the change of variable $s = e_1 - (e_1 - e_3) \text{csc}^2 \psi$, we readily obtain

$$\begin{aligned} \omega'(g_2, g_3) &= i \int_0^{\pi/2} \frac{d\psi}{\sqrt{(e_1 - e_3) - (e_1 - e_2) \sin^2 \psi}} \\ &\equiv \frac{iK(m')}{\sqrt{e_1 - e_3}}, \end{aligned} \tag{B.2}$$

where $m' = 1 - m = (e_1 - e_2)/(e_1 - e_3)$.

Note that the relations (B.1)–(B.2) between the Weierstrass *half*-periods (ω, ω') and the Jacobi *quarter*-periods (K, K') hold because the relation (A.6) between the Weierstrass and Jacobi elliptic functions involves the square of the Jacobi elliptic function, which reduces the latter's period by half (e.g., $\sin^2 \varphi$ has a period of π).

These relations played an important role in the Weierstrass solution of the planar pendulum in section 3.1. Under the transformation $\epsilon \rightarrow \bar{\epsilon} = 2 - \epsilon$ generated by the transformation $\varphi_0 \rightarrow \bar{\varphi}_0 \equiv \pi/2 - \varphi_0$, the Jacobian modulus $m \equiv \epsilon/2$ (in the case (a) of table 2) transforms into the Jacobian modulus $\bar{m} = 1 - \epsilon/2 \equiv m'$ (in the case (b) of table 2), which is the complementary

modulus of case (a). According to equations (B.1) and (B.2), since $\omega_1 \equiv \omega = K(m)$ and $\omega_3 \equiv \omega' = iK'(m) = iK'(m')$ in case (a), in case (b) we find

$$\left. \begin{aligned} \bar{\omega}_1 &= K(\bar{m}) = K'(m) \equiv -i\omega_3 \\ \bar{\omega}_3 &= -iK'(\bar{m}) = -iK(m) \equiv -i\omega_1 \end{aligned} \right\}, \quad (\text{B.3})$$

exactly in agreement with the transformation (46).

References

- [1] Whittaker E T 1937 *A Treatise on the Analytical Dynamics of Particles and Rigid Bodies* 4th edn (New York: Dover)
- [2] Landau L D and Lifshitz E M 1976 *Mechanics* (Amsterdam: Elsevier)
- [3] Taylor J R 2005 *Classical Mechanics* (Sausalito, CA: University Science Books)
- [4] Goldstein H, Poole C and Safko J 2002 *Classical Mechanics* 3rd edn (San Francisco: Addison-Wesley)
- [5] Greenhill A G 1959 *The Applications of Elliptic Functions* (New York: Dover)
- [6] Whittaker E T and Watson G N 1963 *A Course of Modern Analysis* 4th edn (Cambridge: Cambridge University Press)
- [7] Milne-Thomson L M 1965 Jacobi elliptic functions and theta functions *Handbook of Mathematical Functions* ed M Abramowitz and I A Stegun (New York: Dover) chapter 16
- [8] Southard T H 1965 Weierstrass elliptic and related functions *Handbook of Mathematical Functions* ed M Abramowitz and I A Stegun (New York: Dover) chapter 18
- [9] For a shorter version of the present paper (with additional material), see Brizard A J 2009 *An Introduction to Lagrangian Mechanics* (Singapore: World Scientific) appendix B
- [10] Erdős P 2000 *Am. J. Phys.* **68** 888
- [11] For a recent textbook on elliptic functions with applications in physics, see Armitage J V and Eberlein W 2006 *Elliptic Functions* (Cambridge: Cambridge University Press)
- [12] Hartle J B 2003 *Gravity: An Introduction to Einstein's General Relativity* (San Francisco: Addison-Wesley)
- [13] Ryden B 2003 *Introduction to Cosmology* (San Francisco: Addison-Wesley)
- [14] Gratton J and Delellis R 1989 *Am. J. Phys.* **57** 683
- [15] Giambo S, Pantano P and Tucci P 1984 *Am. J. Phys.* **52** 238
- [16] Gardner C S, Greene J M, Kruskal M D and Miura R M 1967 *Phys. Rev. Lett.* **19** 1095
- [17] Olver P J 1986 *Applications of Lie Groups to Differential Equations* (New York: Springer) section 3.2
- [18] Degasperis A 1998 *Am. J. Phys.* **66** 486
- [19] Cervero J M 1986 *Am. J. Phys.* **54** 35
- [20] Critchfield C L 1989 *J. Math. Phys.* **30** 295